BBA - Molecular and Cell Biology of Lipids 1864 (2019) 1103–1108

Contents lists available at ScienceDirect

BBA - Molecular and Cell Biology of Lipids

journal homepage: www.elsevier.com/locate/bbalip

Compromising human skin *in vivo* and *ex vivo* to study skin barrier repair

T. Berkers[a,1], W.A. Boiten[a,1], S. Absalah[a], J. van Smeden[a,2], A.P.M. Lavrijsen[b], J.A. Bouwstra[a,*]

[a] Department of Drug Delivery Technology, Cluster BioTherapeutics, Leiden Academic Centre for Drug Research, Leiden University, Leiden, the Netherlands
[b] Department of Dermatology, Leiden University Medical Centre, Leiden, the Netherlands

ABSTRACT

Ex vivo regenerated stratum corneum (SC) after tape-stripping can be used as a model to study the barrier function of compromised skin. Yet, details about how close the regenerated SC model mimics the lipid properties (*e.g.* lipid composition and lipid ordering) of the *in vivo* situation are not known. Here, we examined using a comprehensive ceramide analysis whether human *ex vivo* regenerated SC showed similar lipid properties as human *in vivo* regenerated SC. Both *in vivo* and *ex vivo* regenerated SC had an altered ceramide subclass composition, with increased percentages of sphingosine-based subclass and decreased percentages of phytosphingosine-based subclass ceramides, a reduced mean ceramide chain length, and a higher percentage of unsaturated ceramides. Overall, regenerated SC *ex vivo* showed more pronounced but similar changes compared to the *in vivo* response. One of the purposes of these models is to use them to mimic compromised skin of inflammatory skin diseases. The altered lipid properties in regenerated SC were comparable to those observed in several inflammatory skin diseases, which makes them a valuable model for the barrier properties in inflammatory skin diseases.

1. Introduction

The main skin barrier function is located in the uppermost epidermal layer, the stratum corneum (SC), consisting of terminally differentiated corneocytes embedded in a lipid matrix [1]. A proper lipid organization and lipid composition in this matrix are important for a well-functioning skin barrier [2–4]. The SC barrier lipids (*e.g.* ceramides (CERs), fatty acids, and cholesterol) are mainly assembled in a dense orthorhombic lateral packing while a smaller lipid fraction adopts a less dense hexagonal packing [5,6]. The SC CER fraction consists of a specific set of CER subclasses defined by their sphingoid base and acyl chain. Both chains can vary in carbon chain length and polar head group, resulting in a wide array of differently structured CER species, see Fig. S2.

Tape-stripped healthy human skin *in vivo* is used as a model to study skin with a compromised barrier. This model has been employed to study several aspects of inflammatory skin diseases [7], to examine the penetration of compounds through the skin [8,9], to increase the bioavailability of topical products in the deeper epidermal layers [10], and to generate a compromised skin barrier to examine the biological processes of skin barrier repair [11–13]. One of these processes is restoring the lipid composition and lipid ordering (lipid properties) in the SC. However, little is known about the effect of barrier disruption by tape-stripping on the lipid properties of the regenerated SC, and whether the regenerated SC lipid properties mimic healthy or diseased skin.

An alternative model to study skin barrier repair is by using stripped *ex vivo* skin which regenerates SC over time in the incubator (skin barrier repair (SkinBaR) model) [14]. Several aspects of the lipid properties of this model have been studied and are known to mimic to some extent the lipid properties of inflammatory skin diseases [14,15]. However, it is unknown to what extent the CER composition of the SkinBaR model reflects that of tape-stripped and regenerated human skin *in vivo*. In the present study we examine whether the SkinBaR model can potentially replace skin barrier repair studies in clinical settings. Therefore, we determined the lipid properties in regenerated SC of the *ex vivo* SkinBaR model and in regenerated SC of *in vivo* tape-stripped skin in detail.

The SC of five skin conditions was examined. SC obtained from healthy *in vivo* control skin and regenerated tape-stripped skin is abbreviated as $Ctrl^{In\text{-}vivo}$ and $Reg^{In\text{-}vivo}$, respectively. SC obtained from *ex vivo* control skin, cultured skin, and regenerated cyanoacrylate-stripped skin is hereafter called $Ctrl^{SkinBaR}$, $Cul^{SkinBaR}$, and $Reg^{SkinBaR}$, see Fig. 1.

The results show that the changes in CER subclass composition and CER chain length of $Reg^{SkinBaR}$ SC reflect those observed in $Reg^{In\text{-}vivo}$ SC.

Abbreviations: AD, atopic dermatitis; C34 CER, ceramide with 34 carbon atoms; CER, ceramide; Ctrl, Control; Cul, Cultured; FTIR, Fourier-transform infrared; LC/MS, liquid chromatography–mass spectrometry; LMM, linear mixed model; MCL, mean ceramide carbon chain length; MuCER, monounsaturated ceramide; Reg, regenerated; SC, stratum corneum; SkinBaR model, skin barrier repair model; TEWL, trans-epidermal water loss

* Corresponding author at: Cluster BioTherapeutics, Leiden Academic Centre for Drug Research, Einsteinweg 55, 2333 CC Leiden, the Netherlands.
E-mail address: bouwstra@lacdr.leidenuniv.nl (J.A. Bouwstra).

[1] Both authors contributed equally to this work.

[2] Current address: Centre for Human Drug Research, Leiden, The Netherlands.

https://doi.org/10.1016/j.bbalip.2019.04.005
Received 23 February 2018; Received in revised form 20 December 2018; Accepted 6 January 2019
Available online 17 April 2019

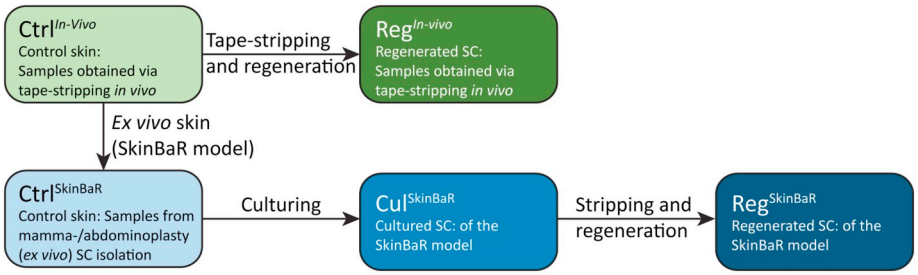

Fig. 1. Explanation of the five different SC samples. The first two conditions were obtained from human *in vivo* skin. The first condition is healthy *in vivo* control skin (hereafter called $Ctrl^{In\text{-}vivo}$). The second condition is tape-stripped and regenereted *in vivo* skin (named $Reg^{In\text{-}vivo}$). The other three conditions were obtained from *ex vivo* skin. These were a control condition for the *ex vivo* skin (called $Ctrl^{SkinBaR}$), non-stripped cultured *ex vivo* skin ($Cul^{SkinBaR}$), and *ex vivo* skin that was stripped and cultured to regenerate the SC ($Reg^{SkinBaR}$).

Both models show that regeneration alters the CER composition and mimics important aspects of the CER composition encountered in inflammatory skin diseases, such as atopic dermatitis (AD).

2. Materials & methods

2.1. Compromised in vivo skin barrier

15 healthy Caucasian volunteers (7 male, 18–29 years) participated in the study. The study was approved by the ethical committee of Leiden University Medical Center and performed according to the Declaration of Helsinki. Volunteers signed written informed consent. To exclude interference with topical products, the volunteers were asked not to use soaps or cosmetics on their ventral forearms during the whole study period. After a 1-week washout period, the SC barrier was disrupted by tape-stripping an area of 3.5 × 2.5 cm on the ventral forearm using D-Squame tape (CuDerm, Dallas, TX). Consecutive tape-strips were used until trans-epidermal water loss (TEWL) values over 60 g/m^2/h were reached and the skin had a shiny appearance [16]. An AquaFlux AF200 (Biox, London, UK) was used to monitor the TEWL. To obtain SC after the 16-day recovery period, 21 tape-strips were harvested at the regenerated site and a control site using polyphenylene sulfide tape (Nichiban, Tokyo, Japan). The first tape-strip (tape 0) was discarded. An infrared spectrum was recorded after each second tape-strip in order to examine the lipid organization (see below).

2.2. Ex vivo human skin (SkinBaR) model

Ex vivo human skin was obtained from a local hospital, used within 12 h after surgery, and handled according to the Declaration of Helsinki principles. The skin was cleaned, processed, stripped, and cultured as described before [14]. SC was isolated and SC sheets were stored over silica gel under argon atmosphere until use for CER extraction or infrared spectroscopy (see below).

2.3. Ceramide analysis by LC/MS

Lipid extraction, liquid chromatography combined with mass spectrometry (LC/MS) measurements, and quantification of tape-strips and SC sheets was performed as described elsewhere [17]. The obtained tape-strips were punched to Ø 16 mm, and extracted using a modified 4 step Bligh and Dyer at 40 °C. Extracts of tapes 5–8 were combined in one sample. After extraction and evaporation of the extraction solvents, samples were dissolved in heptane:chloroform:methanol (95:2.5:2.5) (v:v:v). CERs were analyzed using an Acquity UPLC H-class (Waters, Milford, MA) connected to an XEVO TQ-S mass spectrometer (Waters, Milford, MA). Processing and post-processing were performed as described before [17]. The total molar amount of all CERs was determined quantitatively and used to calculate the molar percentage of each individual CER. The analyzed CER subclasses are depicted in Fig. S2, synthetic CERs that were used for calibration are listed in Table S1.

2.4. SC lipid lateral organization and conformational ordering

Fourier-transform infrared spectroscopy (FTIR) was used to examine the SC lateral lipid organization and the conformational ordering of the SC lipids of *in vivo* and *ex vivo* skin samples [18]. All FTIR spectra were recorded using a Varian 670-IR spectrometer (Agilent Technologies, Santa Clara, CA). For more details, see the Supplementary Methods.

2.5. Statistical analyses

SPSS (v23, IBM, New York, NY) was used for group-wise comparisons using linear mixed models (LMMs) with nested terms. LMMs were used because of the advantages of i) analysis of multiple variables and their interactions in one model, ii) data pairing (*e.g.* multiple conditions within one subject) can be examined, iii) the ability to handle missing data, and iv) the use of nested variables. LMMs were used to examine differences between the $Ctrl^{In\text{-}vivo}$ and $Ctrl^{SkinBaR}$ samples, and the change in the parameter (effect size) of culturing and regeneration of SC. For more details, see Supplementary Methods.

3. Results

To examine if SC regeneration induced changes in CER profile, and whether SC regenerated *ex vivo* was affected differently than SC regenerated *in vivo*, the SC CER composition of the tape-strips obtained in the *in vivo* study and the isolated SC of the SkinBaR model were quantified using a CER lipodomics method, LC/MS. In the present study we quantified the level in each ceramide subclass, (Fig. S2 explains abbreviations used for CERs according to [19]) and calculated the mean carbon chain length (MCL, total number of carbon atoms of the sphingoid base and acyl chain) and the percentage of CERs with a total chain length of 34 carbon atoms (C34 CERs). We focus on these parameters as they correlated with skin barrier function in previous studies [3,13,20,21].

3.1. SC regeneration results in a change in subclass profile and MCL of the CERs

The changes in CER subclass profiles of the 5 different skin conditions were examined. Fig. 2 shows an altered CER profile due to regeneration with similar trends in both $Reg^{In\text{-}vivo}$ and $Reg^{SkinBaR}$ compared to their controls ($Reg^{In\text{-}vivo}$ *vs.* $Ctrl^{In\text{-}vivo}$ and $Reg^{SkinBaR}$ *vs.* $Cul^{SkinBaR}$). Both regenerated models showed increased percentages of S subclass CERs, whereas all three P subclasses and NH subclass CERs were decreased. The percentages of AH subclass CERs were only affected in the $Reg^{SkinBaR}$ samples and not in the $Reg^{In\text{-}vivo}$ samples. No variation in the dS CER subclasses was observed. All CER O subclasses increased in both $Reg^{In\text{-}vivo}$ and $Reg^{SkinBaR}$ samples. Table S2 shows the results of the LMM analysis which indicated that the increased S subclasses and decreased P and NH subclasses in the regenerated SC (both *in vivo* and SkinBaR) compared to their respective controls were statistically significant.

Changes in the percentage of acyl-CERs (EO subclasses) did not show a similar trend, but showed inverse effects in the SkinBaR model

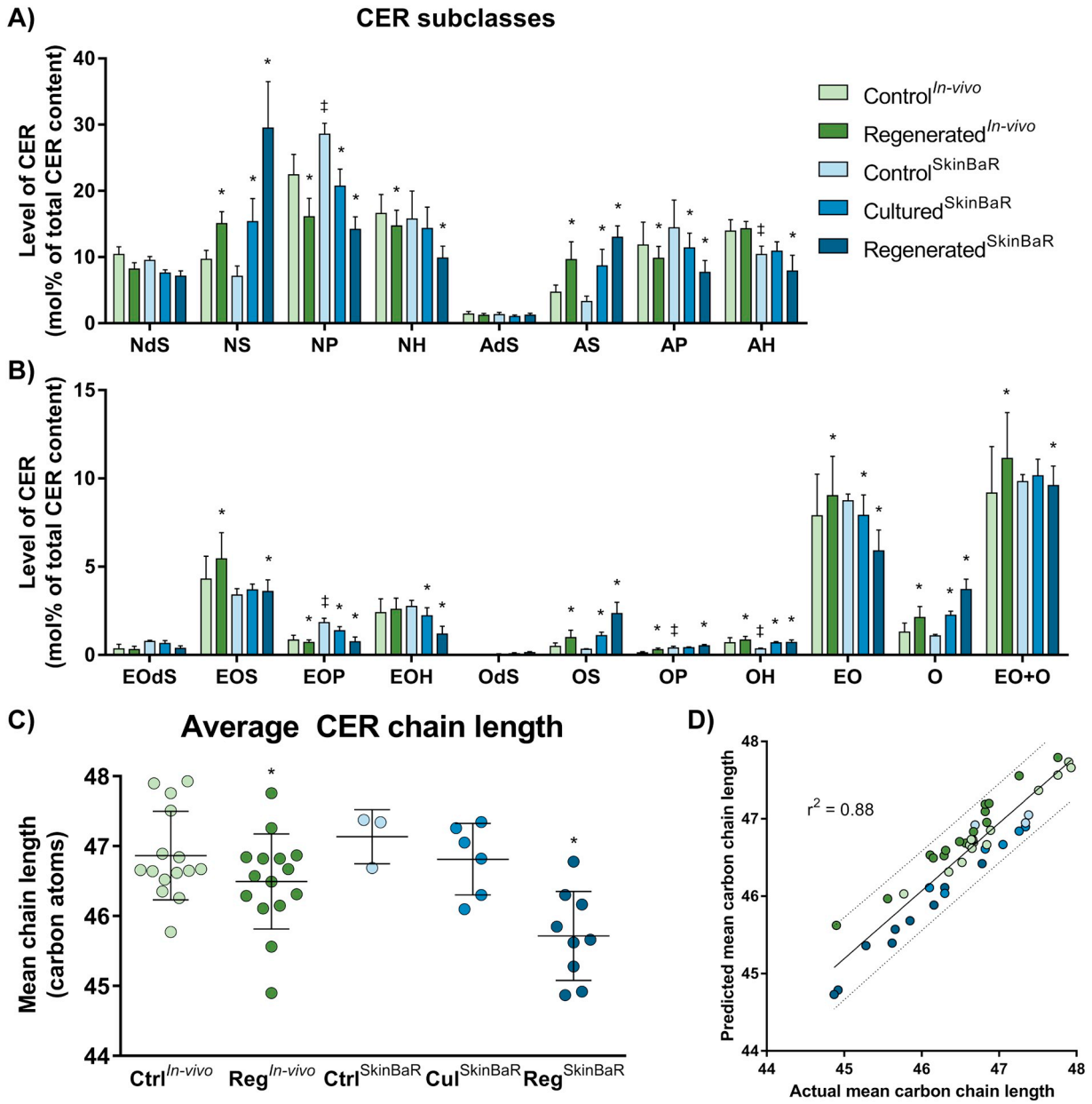

Fig. 2. *In vivo* and SkinBaR model ceramide profiles and mean ceramide chain length show a very similar alteration compared to their controls. A-B) The total molar amount of all CERs was set at 100%. Bars show the CER subclass distribution in molar percentage of the total amount of CERs. $N = 15$ for *in vivo* samples, $N = 3$, 6, and 9 for $Ctrl^{SkinBaR}$, $Cul^{SkinBaR}$ and $Reg^{SkinBaR}$, respectively. C) The MCL of all CERs. D) Correlation of the MCL with the predicted MCL (for residuals: see Fig. S4). Dotted lines: 95% confidence interval. Bars: mean ± SD, $^{*}p < 0.05$ compared to its respective control, ‡ $Ctrl^{SkinBaR}$ is different from $Ctrl^{In\text{-}vivo}$ ($p < 0.05$).

(decrease in percentage of EO subclasses in regenerated SC) compared to *in vivo* skin (increase in percentage EO subclasses in regenerated SC). When the percentages of EO and O CERs within each sample type were combined, there was only a minor difference in total (EO and O) percentage CERs induced by regeneration compared to control (see Fig. 2B and Table S3).

Because the average CER chain length is important for the skin barrier function, the MCL of all CERs was calculated (Fig. 2C and Table S3). In $Ctrl^{In\text{-}vivo}$ skin the CERs had a MCL of 46.9 carbon atoms, and in $Ctrl^{SkinBaR}$ and $Cul^{SkinBaR}$ skin the MCL did not show a significant difference and were 47.1 and 46.8, respectively. Significant reductions in MCL of the CERs, with approximately 0.4 and 1 carbon atom, were observed in the $Reg^{In\text{-}vivo}$ and $Reg^{SkinBaR}$, respectively (Table S4).

3.2. Regenerated SC increased percentage of C34 ceramides and unsaturated ceramides

Another parameter of interest is the fraction of C34 CERs. $Ctrl^{In\text{-}vivo}$ and $Ctrl^{SkinBaR}$ had similar percentages of C34 CERs. Compared to these controls, the mol% C34 CERs was significantly increased due to culturing and regeneration. The effect of regeneration was significantly larger in $Reg^{SkinBaR}$ than in $Reg^{In\text{-}vivo}$ (Fig. S3, Table S5). To determine if the increase in the fraction of C34 CERs was independent of changes in subclass, the percentages of C34s within each subclass was determined. Again, the mol% C34 CERs within subclasses did not significantly differ for $Ctrl^{In\text{-}vivo}$ and $Ctrl^{SkinBaR}$. Within the subclasses, the percentages of C34 CERs were increased in $Cul^{SkinBaR}$ samples compared to the control.

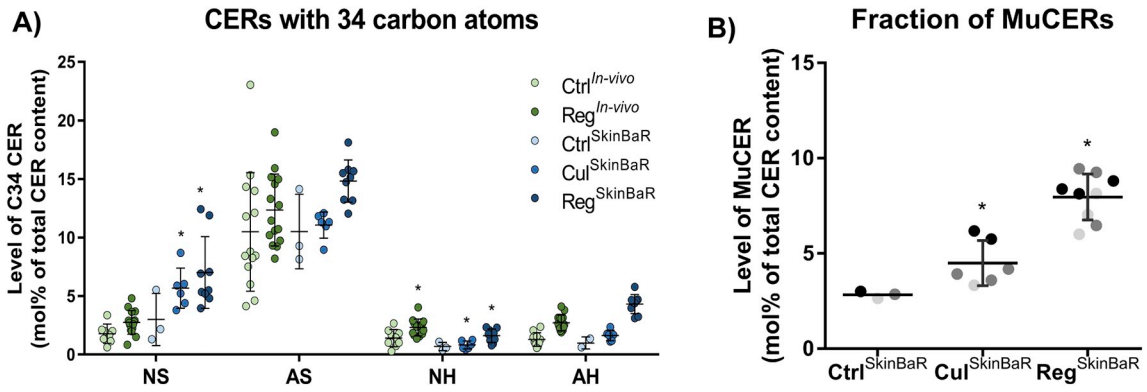

Fig. 3. The percentage of C34 ceramides and unsaturated CERs in the SC increased in the regenerated SC. A) The percentage of C34 per CER subclass. B) The percentage of the monounsaturated CERs in mol%. Data of 3 donors was analyzed, indicated by different shades of gray. Bars: mean ± SD, *$p < 0.05$ compared to its respective control.

Furthermore, in both $Reg^{In\text{-}vivo}$ and $Reg^{SkinBaR}$, a further increase in the percentage of C34 within the subclasses NS, AS, NH, and AH was observed (Fig. 3, Table S5). For the CER subclasses NP, NdS, AP, and AdS a similar increase was observed (Fig. S3). Due to the limited amount of SC acquired by tape-stripping (*in vivo*), C34 percentages of these CER subclasses fall below the detection limit.

As C34 CERs together with EO CERs have been shown to influence the MCL in previous studies, we investigated whether an LMM with the parameters EO CERs and C34 CERs could be used to predict the MCL (Table S6). A high correlation between the predicted and measured MCL was observed (Figure 2D), indicating 88% of the variation in MCL could be explained by the change in percentage EO CERs and C34 CERs.

Another important CER composition parameter is the percentage of mono-unsaturated CERs (MuCERs). Although MuCERs were detected in *in vivo* tape-stripping samples, these could not be accurately determined for all samples. The MuCER percentages of the three SkinBaR sample groups were compared using an LMM (Table S7). In $Ctrl^{SkinBaR}$ SC 2.8 mol% MuCERs were present. This fraction significantly increased to 4.4 mol% in $Cul^{SkinBaR}$ samples ($p = 0.04$) and to 8.0 mol% in $Reg^{SkinBaR}$ SC ($p < 0.01$), see Fig. 3B.

3.3. SC regeneration does not affect lipid ordering

The lipid ordering was analyzed using FTIR. For the SkinBaR samples, CH_2 stretching vibrations in the FTIR spectra could be obtained over a temperature range from 0 to 90 °C. In order to compare the results obtained from the *in vivo* study and the SkinBaR model, the lipid ordering was examined using the center of gravity of the CH_2 symmetric stretching vibration peak in the FTIR spectra of SC at skin temperature (32 °C), see Fig. 4A. A peak position below 2850 cm^{-1} indicates a conformational ordering of the lipids. If the peak position is increased to wavenumbers above 2852 cm^{-1}, the lipids in the SC are mainly in a conformational disordered state, which is a liquid state. In spectra from both $Ctrl^{In\text{-}vivo}$ and $Reg^{In\text{-}vivo}$ samples, the CH_2 peak was positioned at 2848.7 cm^{-1}. For the $Ctrl^{SkinBaR}$ and $Cul^{SkinBaR}$ samples the peak position was located at wavenumbers of 2849.2 cm^{-1} and 2849.3 cm^{-1}, respectively, which was significantly higher than in the spectra of the *in vivo* samples. Although the peak position in the spectra of $Reg^{SkinBaR}$ is substantially higher than that of $Ctrl^{SkinBaR}$, this difference was not statistically significant in the LMM (Table S8).

3.4. Ceramide composition can predict the lipid ordering

Due to the relation between the lipid composition and conformational ordering, the difference between the conformational ordering of the lipids in the SC of the *in vivo* and SkinBaR samples might be explained by changes in lipid composition. To obtain insight in the contribution of parameters related to ceramide composition, these were used to make a predictive model for the lipid ordering (*i.e.* CH_2 stretching peak position). We included ceramide related parameters in an LMM (Table S9). These parameters were i) C34 and EO percentage (together being an MCL predictor), and ii) the subclass molar ratio $\frac{dS+P+H}{S}$ (excluding EO ceramides) which correlated with barrier function in a previous study [17]. For more details about the subclass ratio, see Supplementary Methods. Fig. 4B depicts the actual CH_2-peak position compared to the predicted position. The r^2 indicates that 64% of

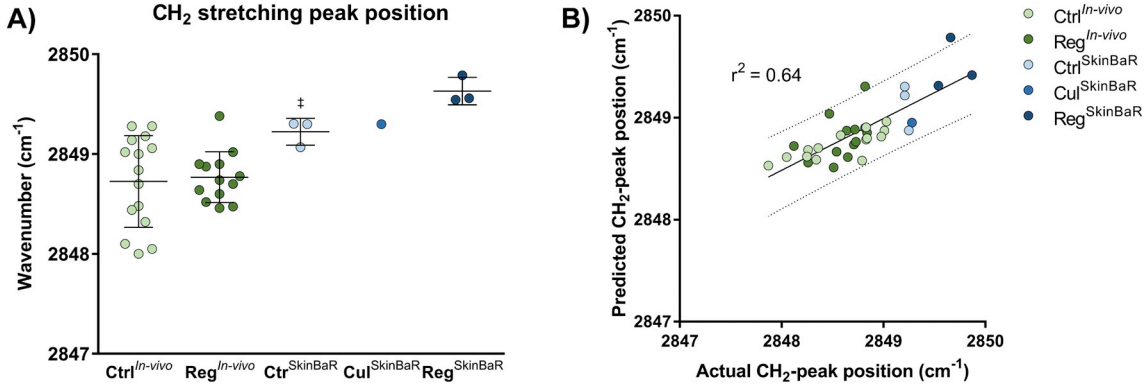

Fig. 4. CH_2 symmetric stretching vibrations in spectra of *in vivo* skin and SkinBaR models and correlation of predicted values for the CH_2 stretching peak with observed values. A) The CH_2 stretching peak positions in the FTIR spectra at skin temperature of 32 °C. Bars: mean ± SD, ‡ $Ctrl^{SkinBaR}$ is different from $Ctrl^{In\text{-}vivo}$ (LMM: $p < 0.05$). B) The linear mixed model used to predict the CH_2 stretching peak includes percentages of C34 CERs and EO CERs, and two CER subclass ratios (for residuals: see Fig. S5). Dotted lines: 95% confidence interval.

the variation in CH_2-peak position was explained, with normally distributed residuals. This model showed that the combination of these CER-related parameters could predict the lipid conformational ordering in SkinBaR and *In vivo* samples.

4. Discussion

An important property of the validity of a skin model is that the model translates to physiological conditions. Here, we examined the translation (to physiological conditions) of the previously developed SkinBaR model [14] to the *in vivo* situation with a focus on the SC lipids.

4.1. CER composition in regenerated SC of SkinBaR model is similar to that in regenerated SC in vivo

In general, the CER percentages and lipid properties in the $Reg^{SkinBaR}$ samples were changed compared to control samples, but resembled those in $Reg^{In\text{-}vivo}$ samples. However, the changes observed in $Reg^{SkinBaR}$ were more pronounced, as discussed below.

i) Both regenerated SC models showed decreased mol% of CER P subclasses and increased percentage of CER S subclasses compared to control SC samples. This indicates an imbalance in activity of the enzymes acid sphingomyelinase and glucocerebrosidase, both involved in post-synthetic modification of CERs [22]. Although the expression of these enzymes was not affected in the SkinBaR model [14], their activity could have been altered [23]. Besides the changes in S and P subclasses, both the $Reg^{SkinBaR}$ and $Reg^{In\text{-}vivo}$ models also showed similarities in a decreased CER MCL, and an increase in percentages of C34 CERs compared to their controls.
ii) The percentage of unsaturated CERs was predominantly increased in $Reg^{SkinBaR}$ SC. In agreement with the elevated percentage of unsaturated CERs, the expression of Stearoyl-CoA desaturase, a lipid processing enzyme responsible for hydrocarbon chain unsaturation, was increased in the SkinBaR model [14].
iii) The only substantial difference between the *in vivo* model and the SkinBaR model was the change in percentages of EO CERs, which was increased in the $Reg^{In\text{-}vivo}$ samples and decreased in the $Reg^{SkinBaR}$ samples.
iv) The lipid ordering was not significantly affected by regeneration in both *in vivo* and *ex vivo* conditions. This might be due to less deep stripping in the present study compared to previous studies. Previously, lipids in the regenerated SC of the SkinBaR model were less ordered when almost all SC was removed [15]. Although the difference in CH_2 stretching peak position between $Ctrl^{In\text{-}vivo}$ and $Ctrl^{SkinBaR}$ was significant, a difference in spectrum collection methods did not play an important role: the CER composition could be used to accurately predict the lipid ordering. Therefore, the difference in peak position mainly originated from a difference in CER composition.

4.2. SC regeneration process in vivo and ex vivo: a comparison

Previously, it has been shown that both in clinical settings and in the SkinBaR model the proliferation rate immediately after barrier disruption is higher than after a recovery period of several days [7,14]. In the SkinBaR model, the proliferation rate was normalized after 8 days of culturing [14], whereas in *in vivo* skin, the proliferation rate remained elevated for at least 10 days [7]. This indicates that there is a difference in velocity at which skin barrier repairs. This may be caused by an inflammatory response in healthy *in vivo* skin during skin barrier repair that slows down the repair process [24]. The fact that the systemic response is lacking in the SkinBaR model substantiates the faster barrier repair process as described above. This also indicates that, during skin barrier repair, the *in vivo* skin is closer to skin homeostasis, which may be an underlying factor for the smaller deviation in changes in CER composition *in vivo* compared to the *ex vivo* SkinBaR model. Since barrier function recovery of stripped healthy human skin takes at least 14 days [25], this period and the period of 8 days in the SkinBaR model are sufficient long to study the effect of formulations on skin barrier repair.

4.3. Modulation in lipid barrier composition in regenerated skin is very similar to that in inflammatory skin diseases

It was shown that tape-stripping healthy skin induced parakeratosis [7], and induced an inflammatory response by secretion of various cytokines [26,27]. Some of these cytokines also play a role in AD and/or psoriasis [28,29] and have been shown to induce changes in the lipid biosynthesis in the viable epidermis, such as a reduction in lipid chain length, also observed in the present study [30,31].

When comparing the lipid properties of regenerated SC to that in SC of inflammatory diseased skin, many similarities were observed. These were i) similar changes in CER subclasses [20], ii) a decreased MCL [32], iii) an increase in percentages of C34 CERs [20,32], and iv) an increased percentage of unsaturated lipids [33]. Most of these changes correlated with an impaired skin barrier function [3,13,20]. Although the degree of changes vary, many of these alterations in CER composition have also been observed in other inflammatory skin diseases like psoriasis, and Netherton syndrome [31,34]. Additionally, a less dense lipid packing observed in $Reg^{SkinBaR}$ SC [15] also corresponds to findings in SC of these inflammatory skin diseases: a higher fraction of lipids adopting a less dense hexagonal lateral packing has been reported [35].

In the present study, we focused on the relation between lipid composition and lipid organization in SC and how changes in the lipid composition in regenerated SC of the SkinBaR model are related to the changes in lipid composition and organization in regenerated SC in a clinical setting. For this study we focused on the composition and organization of the free extractable lipids, yet we acknowledge that the bound ceramides are an important part of the stratum corneum. Analysis of the bound ceramides might be the subject of future studies.

5. Conclusion

This study shows that the changes in lipid properties in both the $Reg^{SkinBaR}$ and $Reg^{In\text{-}vivo}$ models are very similar and mimic the lipid properties in inflammatory skin diseases. This concerns changes in CER subclass profiles, MCL, percentage of CER unsaturation, and conformational ordering. Therefore, the SkinBaR model can be used to predict the *in vivo* response with regards to the lipid composition after application of topical barrier repair treatments aiming to restore the normal CER composition. By doing so, the need for clinical studies is reduced.

Conflict of interest

The authors state no conflict of interest.

Transparency document

The Transparency document associated this article can be found, in online version.

Acknowledgement

The authors would like acknowledge Gert Gooris for his help with programming the FTIR method. The authors express their gratitude to Evonik for supplying the synthetic CERs. This research was financially supported by Dutch Technology Foundation TTW (grant no. 12400).

Appendix A. Supplementary data

Supplementary data to this article can be found online at https://doi.org/10.1016/j.dummy.2019.01.002.

References

[1] A.S.C. Michaels, S. K., J.E. Shaw, Drug permeation through human skin – theory and in vitro experimental measurement, Am. Inst. Chem. Eng. J. 21 (1975) 12.

[2] E.H. Mojumdar, Z. Kariman, L. van Kerckhove, G.S. Gooris, J.A. Bouwstra, The role of ceramide chain length distribution on the barrier properties of the skin lipid membranes, Biochim. Biophys. Acta 1838 (2014) 2473–2483.

[3] M. Janssens, J. van Smeden, G.S. Gooris, W. Bras, G. Portale, P.J. Caspers, R.J. Vreeken, T. Hankemeier, S. Kezic, R. Wolterbeek, A.P. Lavrijsen, J.A. Bouwstra, Increase in short-chain ceramides correlates with an altered lipid organization and decreased barrier function in atopic eczema patients, J. Lipid Res. 53 (2012) 2755–2766.

[4] S. Stahlberg, S. Lange, B. Dobner, D. Huster, Probing the role of ceramide headgroup polarity in short-chain model skin barrier lipid mixtures by (2)H solid-state NMR spectroscopy, Langmuir 32 (2016) 2023–2031.

[5] G.S. Pilgram, A.M. Engelsma-van Pelt, J.A. Bouwstra, H.K. Koerten, Electron diffraction provides new information on human stratum corneum lipid organization studied in relation to depth and temperature, J. Invest. Dermatol. 113 (1999) 403–409.

[6] F. Damien, M. Boncheva, The extent of orthorhombic lipid phases in the stratum corneum determines the barrier efficiency of human skin in vivo, J. Invest. Dermatol. 130 (2010) 611–614.

[7] M.J. Gerritsen, P.E. van Erp, I.M. van Vlijmen-Willems, L.T. Lenders, P.C. van de Kerkhof, Repeated tape stripping of normal skin: a histological assessment and comparison with events seen in psoriasis, Arch. Dermatol. Res. 286 (1994) 455–461.

[8] X. Wu, B. Biatry, C. Cazeneuve, R.H. Guy, Drug delivery to the skin from sub-micron polymeric particle formulations: influence of particle size and polymer hydrophobicity, Pharm. Res. 26 (2009) 1995–2001.

[9] Y. Gao, X. Wang, S. Chen, S. Li, X. Liu, Acute skin barrier disruption with repeated tape stripping: an in vivo model for damage skin barrier, Skin Res. Technol. 19 (2013) 162–168.

[10] H. Dickel, A. Goulioumis, T. Gambichler, J.W. Fluhr, J. Kamphowe, P. Altmeyer, O. Kuss, Standardized tape stripping: a practical and reproducible protocol to uniformly reduce the stratum corneum, Skin Pharmacol. Physiol. 23 (2010) 259–265.

[11] R. Ghadially, B.E. Brown, S.M. Sequeira-Martin, K.R. Feingold, P.M. Elias, The aged epidermal permeability barrier. Structural, functional, and lipid biochemical abnormalities in humans and a senescent murine model, J. Clin. Invest. 95 (1995) 2281–2290.

[12] M.G. Williams, R. Hunter, Studies on epidermal regeneration by means of the strip method, J. Invest. Dermatol. 29 (1957) 407–413.

[13] W.A. Boiten, T. Berkers, S. Absalah, J. van Smeden, A.P.M. Lavrijsen, J.A. Bouwstra, Applying a vernix caseosa based formulation accelerates skin barrier repair by modulating lipid biosynthesis, J. Lipid Res. 59 (2018) 250–260.

[14] M.O. Danso, T. Berkers, A. Mieremet, F. Hausil, J.A. Bouwstra, An ex vivo human skin model for studying skin barrier repair, Exp. Dermatol. 24 (2015) 48–54.

[15] T. Berkers, D. Visscher, G.S. Gooris, J.A. Bouwstra, Degree of skin barrier disruption affects lipid organization in regenerated stratum corneum, Acta Derm. Venereol. 98 (2018) 421–427.

[16] H. Pinkus, Examination of the epidermis by the strip method of removing horny layers. I. Observations on thickness of the horny layer, and on mitotic activity after stripping, J. Invest. Dermatol. 16 (1951) 383–386.

[17] W. Boiten, S. Absalah, R. Vreeken, J. Bouwstra, S.J. van, Quantitative analysis of ceramides using a novel lipidomics approach with three dimensional response modelling, Biochim. Biophys. Acta 1861 (2016) 1652–1661.

[18] M. Boncheva, F. Damien, V. Normand, Molecular organization of the lipid matrix in intact stratum corneum using ATR-FTIR spectroscopy, Biochim. Biophys. Acta 1778 (2008) 1344–1355.

[19] S. Motta, M. Monti, S. Sesana, R. Caputo, S. Carelli, R. Ghidoni, Ceramide composition of the psoriatic scale, Biochim. Biophys. Acta 1182 (1993) 147–151.

[20] J. Ishikawa, H. Narita, N. Kondo, M. Hotta, Y. Takagi, Y. Masukawa, T. Kitahara, Y. Takema, S. Koyano, S. Yamazaki, A. Hatamochi, Changes in the ceramide profile of atopic dermatitis patients, J. Invest. Dermatol. 130 (2010) 2511–2514.

[21] G. Grubauer, K.R. Feingold, R.M. Harris, P.M. Elias, Lipid content and lipid type as determinants of the epidermal permeability barrier, J. Lipid Res. 30 (1989) 89–96.

[22] Y. Uchida, M. Hara, H. Nishio, E. Sidransky, S. Inoue, F. Otsuka, A. Suzuki, P.M. Elias, W.M. Holleran, S. Hamanaka, Epidermal sphingomyelins are precursors for selected stratum corneum ceramides, J. Lipid Res. 41 (2000) 2071–2082.

[23] J. van Smeden, I.M. Dijkhoff, R.W.J. Helder, H. Al-Khakany, D.E.C. Boer, A. Schreuder, W.W. Kallemeijn, S. Absalah, H.S. Overkleeft, J. Aerts, J.A. Bouwstra, In situ visualization of glucocerebrosidase in human skin tissue: zymography versus activity-based probe labeling, J. Lipid Res. 58 (2017) 2299–2309.

[24] T.K. Lin, L. Zhong, J.L. Santiago, Anti-inflammatory and skin barrier repair effects of topical application of some plant oils, Int. J. Mol. Sci. 19 (2017).

[25] M. Tanaka, Y.X. Zhen, H. Tagami, Normal recovery of the stratum corneum barrier function following damage induced by tape stripping in patients with atopic dermatitis, Br. J. Dermatol. 136 (1997) 966–967.

[26] H. Dickel, T. Gambichler, J. Kamphowe, P. Altmeyer, M. Skrygan, Standardized tape stripping prior to patch testing induces upregulation of Hsp90, Hsp70, IL-33, TNF-alpha and IL-8/CXCL8 mRNA: new insights into the involvement of 'alarmins', Contact Dermatitis 63 (2010) 215–222.

[27] B.J. Nickoloff, Y. Naidu, Perturbation of epidermal barrier function correlates with initiation of cytokine cascade in human skin, J. Am. Acad. Dermatol. 30 (1994) 535–546.

[28] E. Ogawa, Y. Sato, A. Minagawa, R. Okuyama, Pathogenesis of psoriasis and development of treatment, J. Dermatol. 45 (2017) 264–272.

[29] A. Kouris, A. Pistiki, A. Katoulis, M. Georgitsi, S. Giatrakou, E. Papadavid, M.G. Netea, N. Stavrianeas, E.J. Giamarellos-Bourboulis, Proinflammatory cytokine responses in patients with psoriasis, Eur. Cytokine Netw. 25 (2014) 63–68.

[30] M.O. Danso, V. van Drongelen, A. Mulder, J. van Esch, H. Scott, J. van Smeden, A. El Ghalbzouri, J.A. Bouwstra, TNF-alpha and Th2 cytokines induce atopic dermatitis-like features on epidermal differentiation proteins and stratum corneum lipids in human skin equivalents, J. Invest. Dermatol. 134 (2014) 1941–1950.

[31] C. Tawada, H. Kanoh, M. Nakamura, Y. Mizutani, T. Fujisawa, Y. Banno, M. Seishima, Interferon-gamma decreases ceramides with long-chain fatty acids: possible involvement in atopic dermatitis and psoriasis, J. Invest. Dermatol. 134 (2014) 712–718.

[32] J. van Smeden, J.A. Bouwstra, Stratum corneum lipids: their role for the skin barrier function in healthy subjects and atopic dermatitis patients, Curr. Probl. Dermatol. 49 (2016) 8–26.

[33] J. van Smeden, M. Janssens, E.C. Kaye, P.J. Caspers, A.P. Lavrijsen, R.J. Vreeken, J.A. Bouwstra, The importance of free fatty acid chain length for the skin barrier function in atopic eczema patients, Exp. Dermatol. 23 (2014) 45–52.

[34] J. van Smeden, M. Janssens, W.A. Boiten, V. van Drongelen, L. Furio, R.J. Vreeken, A. Hovnanian, J.A. Bouwstra, Intercellular skin barrier lipid composition and organization in Netherton syndrome patients, J. Invest. Dermatol. 134 (2014) 1238–1245.

[35] J. van Smeden, M. Janssens, G.S. Gooris, J.A. Bouwstra, The important role of stratum corneum lipids for the cutaneous barrier function, Biochim. Biophys. Acta 1841 (2014) 295–313.